



HAL
open science

Interaction of dense shelf water cascading and open-sea convection in the northwestern Mediterranean during winter 2012

Xavier Durrieu de Madron, Loïc Houpert, Pere Puig, A. Sanchez-Vidal, Pierre Testor, Anthony Bosse, Claude Estournel, S Somot, François Bourrin, Marie-Noëlle Bouin, et al.

► To cite this version:

Xavier Durrieu de Madron, Loïc Houpert, Pere Puig, A. Sanchez-Vidal, Pierre Testor, et al.. Interaction of dense shelf water cascading and open-sea convection in the northwestern Mediterranean during winter 2012. *Geophysical Research Letters*, 2013, 40 (7), pp.1379-1385. 10.1002/GRL.50331 . hal-00873390

HAL Id: hal-00873390

<https://hal.science/hal-00873390v1>

Submitted on 9 Apr 2021

HAL is a multi-disciplinary open access archive for the deposit and dissemination of scientific research documents, whether they are published or not. The documents may come from teaching and research institutions in France or abroad, or from public or private research centers.

L'archive ouverte pluridisciplinaire **HAL**, est destinée au dépôt et à la diffusion de documents scientifiques de niveau recherche, publiés ou non, émanant des établissements d'enseignement et de recherche français ou étrangers, des laboratoires publics ou privés.

Interaction of dense shelf water cascading and open-sea convection in the northwestern Mediterranean during winter 2012

X. Durrieu de Madron,¹ L. Houpert,¹ P. Puig,² A. Sanchez-Vidal,³ P. Testor,⁴ A. Bosse,⁴ C. Estournel,⁵ S. Somot,⁶ F. Bourrin,¹ M. N. Bouin,⁷ M. Beauverger,⁴ L. Beguery,⁸ A. Calafat,³ M. Canals,³ C. Cassou,⁹ L. Coppola,¹⁰ D. Dausse,⁴ F. D'Ortenzio,¹⁰ J. Font,² S. Heussner,¹ S. Kunesch,¹ D. Lefevre,¹¹ H. Le Goff,⁴ J. Martín,² L. Mortier,⁴ A. Palanques,² and P. Raimbault¹¹

Received 2 January 2013; revised 4 March 2013; accepted 6 March 2013; published 15 April 2013.

[1] The winter of 2012 experienced peculiar atmospheric conditions that triggered a massive formation of dense water on the continental shelf and in the deep basin of the Gulf of Lions. Multiplatforms observations enabled a synoptic view of dense water formation and spreading at basin scale. Five months after its formation, the dense water of coastal origin created a distinct bottom layer up to a few hundreds of meters thick over the central part of the NW Mediterranean basin, which was overlaid by a layer of newly formed deep water produced by open-sea convection. These new observations highlight the role of intense episodes of both dense shelf water cascading and open-sea convection to the progressive modification of the NW Mediterranean deep waters. **Citation:** Durrieu de Madron, X., et al. (2013), Interaction of dense shelf water cascading and open-sea convection in the northwestern Mediterranean during winter 2012, *Geophys. Res. Lett.*, 40, 1379–1385, doi:10.1002/grl.50331.

1. Introduction

[2] Dense shelf water cascading and open-sea convection coexist in a few regions around the world such as the Mediterranean (Gulf of Lions, Adriatic Sea, Aegean Sea)

¹CEFREM, CNRS-Université de Perpignan, 52 avenue Paul Alduy, 66860, Perpignan, France.

²ICM-CSIC, Passeig Marítim de la Barceloneta, 37-49, 08003, Barcelona, Spain.

³GRC-GM, Universitat de Barcelona, Martí i Franquès s/n, 08028, Barcelona, Spain.

⁴LOCEAN/IPSL, CNRS-Université de Paris 6, 4 Place Jussieu, 75005, Paris, France.

⁵LA, CNRS-Université de Toulouse, 14 avenue Edouard Belin, 31400, Toulouse, France.

⁶CNRM-GAME, Météo France - CNRS, 42 avenue Coriolis, 31057, Toulouse, France.

⁷CMM, Météo-France, 13 rue du Chatellier, 29604, Brest, France.

⁸DT-INSU, CNRS, Zone portuaire de Breguailon, 83507, La Seyne/mer, France.

⁹CERFACS/CNRS, 42 avenue Gaspard Coriolis, 31057, Toulouse, France.

¹⁰LOV, CNRS-Université de Paris 6, Observatoire océanographique, 06234, Villefranche/mer, France.

¹¹MIO, CNRS-Université de la Méditerranée, Campus de Luminy, 13288, Marseille, France.

Corresponding author: X. Durrieu de Madron, CEFREM, CNRS-Université de Perpignan, 52 ave. Paul Alduy, 66860 Perpignan, France. (demadron@univ-perp.fr)

[CIESM, 2009], the East/Japan Sea [Kim et al., 2008], and Greenland Sea [Quadfasel et al., 1988]. However, interplay between both types of processes on the deep water mass characteristics is still poorly documented.

[3] In the Gulf of Lions (GoL), dense water formation shows a high interannual variability. It is mostly produced by surface cooling and evaporation due to cold and dry northern winds, and preconditioning of the water column. Dense shelf water overflowing the shelf edge occasionally cascades down to more than 2000 m, resulting in the apparition of fresher and colder bottom water in the basin [Canals et al., 2006; Font et al., 2007]. Open-sea convection involves a progressive deepening of the upper ocean mixed layer, which first reaches the warmer and saltier underlying Levantine Intermediate Water and eventually extends all the way down to the bottom, should the atmospheric forcing be intense enough [L'Heveder et al., 2012].

[4] Although open-sea convection is the main mechanism for the renewal of the Western Mediterranean Deep Water (WMDW), the influence of dense shelf water cascading has been suggested by several studies. Analysis of historical temperature-salinity profiles from the late 1960s suggested mixing of deep cascading and convection dense waters, with a subdecadal recurrence [Béthoux et al., 2002], the winters 2005 and 2006 being the last major events [Puig et al., 2013].

[5] Here we present a comprehensive set of hydrological and hydrodynamical observations collected during the winter and summer 2012 that provide new insights on the propagation and mixing of both type of the dense shelf waters, and their influence on the modification of the WMDW, as a new step in the Western Mediterranean Transition that started in 2005 [CIESM, 2009].

2. Data and Methods

[6] Six mooring lines and two surface buoys constituted the observational design (Figure 1a). Three moorings were located at 1000 m depth in canyons at the NE (Planier, PLC) and SW ends (Lacaze-Duthiers, LDC; Cap de Creus, CCC) of the GoL margin, and three others between 1900–2500 m depth on the Catalan continental slope (HC, FOFA) and GoL basin (LION). Two meteorological buoys were located on the GoL inner shelf of the (POEM), and in the basin (MF-LION).

[7] All the lines were equipped with current meters between 20 and 45 m above bottom, and the deepest ones

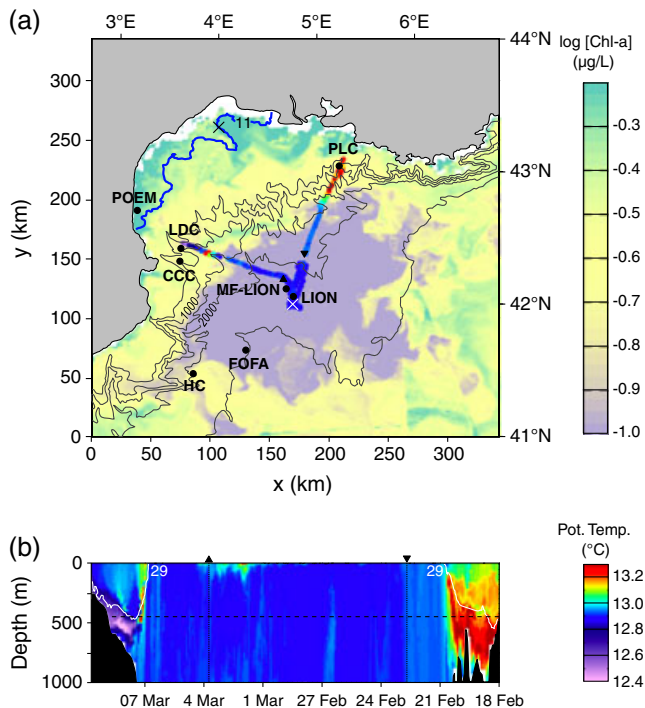


Figure 1. (a) Position of the moorings in the Planier (PLC), Lacaze-Duthiers (LDC), Cap de Creus (CCC) canyons, on the Catalan continental slope (HC, FOFA), and in the basin (LION), and of the surface buoys (POEM, MF-LION). Pale color patterns represent the surface Chlorophyll-*a* concentrations on 22 February 2012 derived from MODIS satellite image. The solid blue line on the shelf shows the offshore extension of the coldest surface water ($< 11^{\circ}\text{C}$) extracted from satellite-derived sea surface temperature on 22 February 2012. The V-shaped track represents the glider section performed between 19 February and 9 March 2012, and colors correspond to the potential temperature at 450 m depth. (b) Section of potential temperature (color) between the surface and 1000 m depth (or the bottom) along the glider section. The 29 kg m^{-3} isopycnal (white line) is superimposed. The horizontal dashed line indicates 450 m depth. Black triangles correspond to the reference points along the section.

also had a conductivity-temperature-depth (CTD) sensor. The line on the GoL basin, which extended from the seafloor to 150 m below sea surface, included 5 current meters, 11 CTD sensors regularly spaced along the line, and 10 supplemental temperature sensors above 650 m depth. Both buoys had a CTD sensor just below the surface, and the offshore buoy had also a thermistor string with 20 sensors between 2 and 200 m depth. The recording period lasted from December 2011 to June 2012.

[8] Winter CTD data were collected between the surface and 1000 m deep with a Sea Glider deployed along a repeat-section in the GoL (Figure 1). A cruise (MOOSE 2012) was conducted in late July 2012 to perform an extensive CTD survey of the NW Mediterranean basin.

[9] ERA-Interim reanalysis of atmospheric heat fluxes were collected from the European Centre for Medium-Range Weather Forecasts. We considered the modeled net heat fluxes from one grid point on the shelf and the closest grid point to the offshore buoy (see X marks in Figure 1a).

[10] Merged product of Moderate Resolution Imaging Spectroradiometer (MODIS) and Operational Sea surface Temperature and sea-Ice Analysis (OSTIA) sea surface temperature was provided by ACRI-ST (<http://www.acri-st.fr>). MODIS ocean color observations of the surface chlorophyll-*a* (OC5 Chl-*a* products) were provided by the MyOcean project (<http://www.myocean.eu/>).

3. Results and Discussion

3.1. Atmospheric Conditions

[11] The winds measured at the offshore buoy from mid-December 2011 to mid-March 2012 showed frequent N-NW wind storms with speed $\geq 20 \text{ m s}^{-1}$ (Figure 2a). Several episodes of strong net heat loss both on the shelf and in the basin occurred in late December 2011 to early January 2012, and during the first two weeks of February 2012 (Figure 2b).

[12] Winter 2012 (i.e., December 2011 to February 2012) can be considered as exceptional over the North Atlantic and Europe region. Following *Cassou et al.* [2010], the daily atmospheric synoptic circulation for this region can be described by four main weather regimes: the negative (NAO-) and positive (NAO+) phases of the North Atlantic Oscillation, the Blockage (BL), and the Atlantic Ridge (AR). During a normal winter (DJF), the duration for each weather regime is respectively 20, 26, 23, and 22 days. However, during winter 2012, no day of NAO- was observed, whereas 44 days (+100%) of AR occurred. NAO+ and BL were closer to normal statistics. The AR regime is characterized by an anticyclonic anomaly in the North Atlantic and a cyclonic anomaly over the Baltic Sea, which is particularly favorable to strong, cold, and dry northerly winds over the GoL enhancing air-sea heat fluxes. During winter 2012, six periods could be identified with at least four consecutive days of AR conditions: 17–20 December, 4–14 January, 19–26 January, 2–5 February, 10–20 February, and 23–26 February. These episodes match well with the strong wind and intense heat loss events over the GoL (Figures 2a and 2b). It is worth to note that the AR pattern (based on daily weather regimes obtained by *k*-means objective classification) looks very similar to the negative phase of the East Atlantic pattern identified by *Josey et al.*, [2011] (based on monthly-mean climate pattern obtained by EOF techniques). Since 1958, the winters (DJF) with large positive anomalies of the number of AR days (at least +25%) and large negative anomalies of the number of NAO- days (at least -25%) were: 1966–1967, 1972–1973, 1975–1976, 1980–1981, 1998–1999, 1999–2000, 2004–2005, and 2011–2012. Most of these winters correspond to years when thermo-haline anomalies indicative of intense shelf and open-sea convections were observed in the basin [*Béthoux et al.*, 2002; *Puig et al.*, 2013]

3.2. Formation of Dense Water on the Shelf and Cascading Along the Continental Slope

[13] The winter heat loss induced a significant cooling of surface water (Figure 2c), especially on the inner and midshelf (Figure 1a). Temperature on the inner shelf was below 10°C during most of February, and fell to a minimum of 8°C on 13 February 2012 (Figure 2c). With this temperature and a salinity of 38.10, the potential density anomaly of the dense shelf water reached 29.710 kg m^{-3} , which exceeded

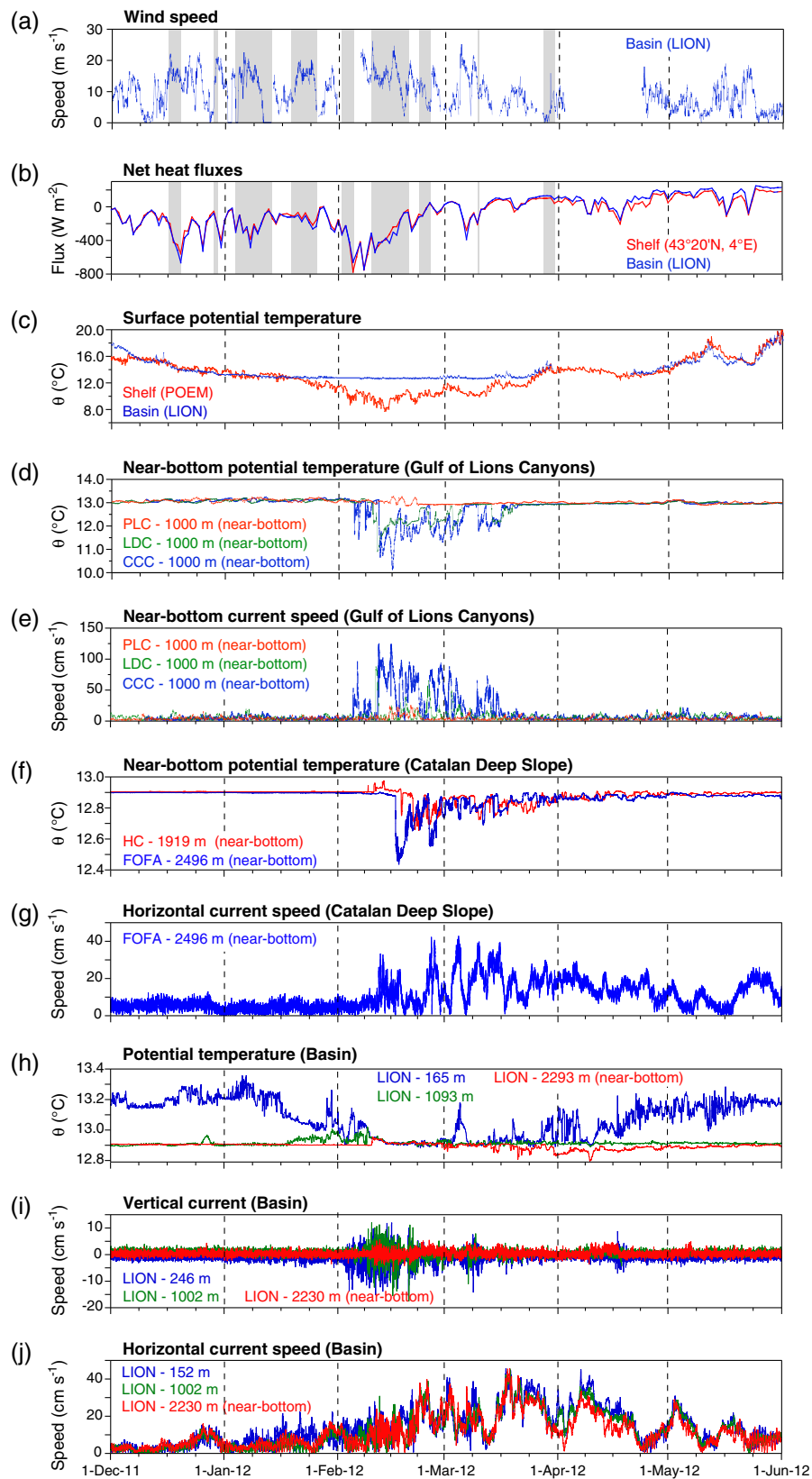


Figure 2. Time series of wind speed, net heat fluxes, potential temperature, and currents between 1 December 2011 and 1 June 2012. (a) Wind speed in the basin, (b) net heat fluxes on the shelf and in the basin, (c) near-surface temperature on the shelf and in the basin, (d) near-bottom temperature at 1000 m depth in the canyons of the GoL, (e) near-bottom horizontal current speed at 1000 m depth in the canyons of the GoL, (f) near-bottom temperature on the deep slope, (g) near-bottom horizontal current speed in the basin, (h) temperature at different depths in the basin, (i) vertical current speeds at different depths in the basin, and (j) horizontal current speed at different depths in the basin. Grey bands show the periods of AR weather regime.

the maximum density of the deep basin prior to the winter 2012 (29.126 kg m^{-3}).

[14] The signature of dense water cascading in the GoL canyons was clearly visible through the temperature drop associated with strong downcanyon currents. While the eastern PLC did not exhibit significant changes, the southwestern LDC and CCC showed from 5 February 2012 to mid-March 2012 several episodes of dense shelf water cascading beyond 1000 m deep with a sharp temperature drop of 1 to 3°C (Figure 2d) and currents up to 125 cm s^{-1} (Figure 2e). The cascading started earlier and was stronger in the CCC. The main cascading episode on 11 February 2012 was concomitant with the appearance of the coldest and densest water on the shelf (Figure 2c). A bottom plume of cold dense water about 200 m thick was visible in early March on the western end of the glider section along the LDC (Figure 1b).

[15] The first anomaly reached the deep slope about 5 days after the main episode of dense water cascading off the GoL shelf. At 1900 m depth on the Catalan slope, a brief temperature drop of 0.15°C , indicating the passage of dense coastal waters was observed on 18 February 2012, while at ~ 2500 m depth, the appearance of dense coastal waters was stronger (drop of 0.45°C) and earlier (16 February 2012) (Figure 2f). For both sites the temperature drops lasted until the beginning of April 2012.

[16] Farther northeast in the basin, the signal of dense shelf water reached (~ 2350 m depth) on 28 February 2012 (Figure 2h), and was delineated by potential temperature $\leq 12.905^\circ\text{C}$ and density anomaly $\geq 29.13 \text{ kg m}^{-3}$ corresponding to the horizontal cusp on the Theta-S curves (Figure 3). The temperature drops (up to 0.1°C) were primarily perceived near the bottom (last few hundred meters above the seabed). However, on some occasions, the negative thermal anomaly reached shallower levels of the water column, indicating the passage of plumes of dense shelf water of variable thickness. On 2–3 March 2012, and on 9–10 April 2012, remarkable anomalies were visible between the bottom and 1000 m depth (Figure 3). The maximum density of the new bottom water at the basin site reached 29.135 kg m^{-3} .

3.3. Formation of Dense Water in the Open Sea

[17] The winter heat losses in the basin cooled the surface layer down to 12.6°C (Figure 2c). At the basin site, strong vertical mixing was evidenced by high frequency vertical velocities of about $\pm 10 \text{ cm s}^{-1}$ (Figure 2i). The thickening of the mixed layer started in December 2011, reaching the Levantine Intermediate Water layer (characterized by a relative maximum temperature and salinity between 200 and 700 m depth, Figure 3) around mid-January 2012 and deepened rapidly to reach the seabed at 2350 m on 10 February 2012, provoking an increase of the near-bottom temperature and salinity (Figures 2h and 3). Between 10 and 17 February 2012, the sustained surface heat loss produced a supplementary cooling of the mixed water column of 0.04°C with no significant change of salinity. Hence, with a potential temperature of 12.905°C and a salinity of 38.508, the maximum density of the new deep water formed by open-sea convection at the basin site reached 29.134 kg m^{-3} (Figure 3). It eventually formed a deep layer, whose upper limit was identified with the isopycnal 29.126 kg m^{-3} (maximum bottom density encountered at the three deep sites prior to the convection period), overlying the bottom water layer (Figure 3).

[18] The surface signature of the convection zone was recognized by a minimum surface chlorophyll concentration ($< 0.1 \mu\text{g L}^{-1}$, Figure 1a). The temperature and density distribution along the glider section across the northern half of the GoL basin confirmed the extension of the convection area down to 1000 m deep (Figure 1b). These observations suggest that the region of intense vertical mixing extended over a large (~ 70 km radius) area, with the basin site being in the central part, and the deep slope sites being on the periphery. The open-ocean convection signal was sensed at the 1900 m site as a slight increase of near-bottom temperature preceding the arrival of cold dense shelf water, but it barely reached the 2500 m site. (Figure 2f).

3.4. Propagation of Newly Formed Deep and Bottom Water in the Deep Basin

[19] Horizontal currents at the basin site were mostly barotropic and isotropic. Current speeds increased at the onset of newly deep waters advent, reaching maximum of 30 to 40 cm s^{-1} during March and April, and decreasing afterward (Figure 2j). At the deep slope site, the period of strongest current speed was shorter (from mid-February to mid-March) and coincided with the cascading period (Figure 2g). At both sites, the currents presented large fluctuations around 2–15 days due to strong eddies contributing to the spreading of the newly-formed deep water, as shown by *Testor and Gascard* [2006].

[20] The progressive spreading of the newly formed water by open-sea convection during the restratification period generated a ~ 300 m thick layer, overlying bottom dense waters of coastal origin, ~ 150 m thick (Figure 3). The extent and thickness of the newly formed deep and bottom waters remaining in the GoL and Ligurian basins in summer showed that the combination of the two layers formed a dome-shaped lens, with a maximum total thickness of 520 m (average 206 m) embracing the winter convection region (Figure 4a). The new deep water layer's thickness averaged 110 m, whereas the layer of new bottom water was thinner and averaged 96 m. However, the summer survey evidenced the presence of two isolated stations on the western part of the lens with anomalous bottom water extending 1100 m above the seafloor (points d and e in Figure 4), likely indicative of eddies.

3.5. Volume Estimates

[21] The estimated volume of dense ($\geq 29.126 \text{ kg m}^{-3}$) water formed by open-sea convection during the winter 2012, considering thickness of the mixed patch ~ 2.2 km and a surface of $\sim 15,500 \text{ km}^2$ (horizontal extent with chl-*a* concentration $\leq 0.1 \mu\text{g L}^{-1}$, Figure 1a), amounted to about $34,100 \text{ km}^3$, which corresponds to an annual mean flux of $\sim 1.1 \times 10^6 \text{ m}^3 \text{ s}^{-1}$. This flux is close to the mean production rate for the two winters 2005 and 2006 ($\sim 2.40 \times 10^6 \text{ m}^3 \text{ s}^{-1}$) estimated by *Schroeder et al.* [2008]. The flux of dense shelf water cascading down the CCC, which concentrates about half the total volume of dense shelf water exported beyond 1000 m depth according to *Ulses et al.* [2008], was approximated using the observed current speed associated with water colder than ambient water (i.e., $\theta \leq 12.92^\circ\text{C}$), and a plume cross-section of 200 m thick (inferred from Figure 1b) and 4 km wide (local canyon width). The cascading period accounted 43 days with a mean downcanyon speed of 36.6 cm s^{-1} , and the volume of dense shelf water

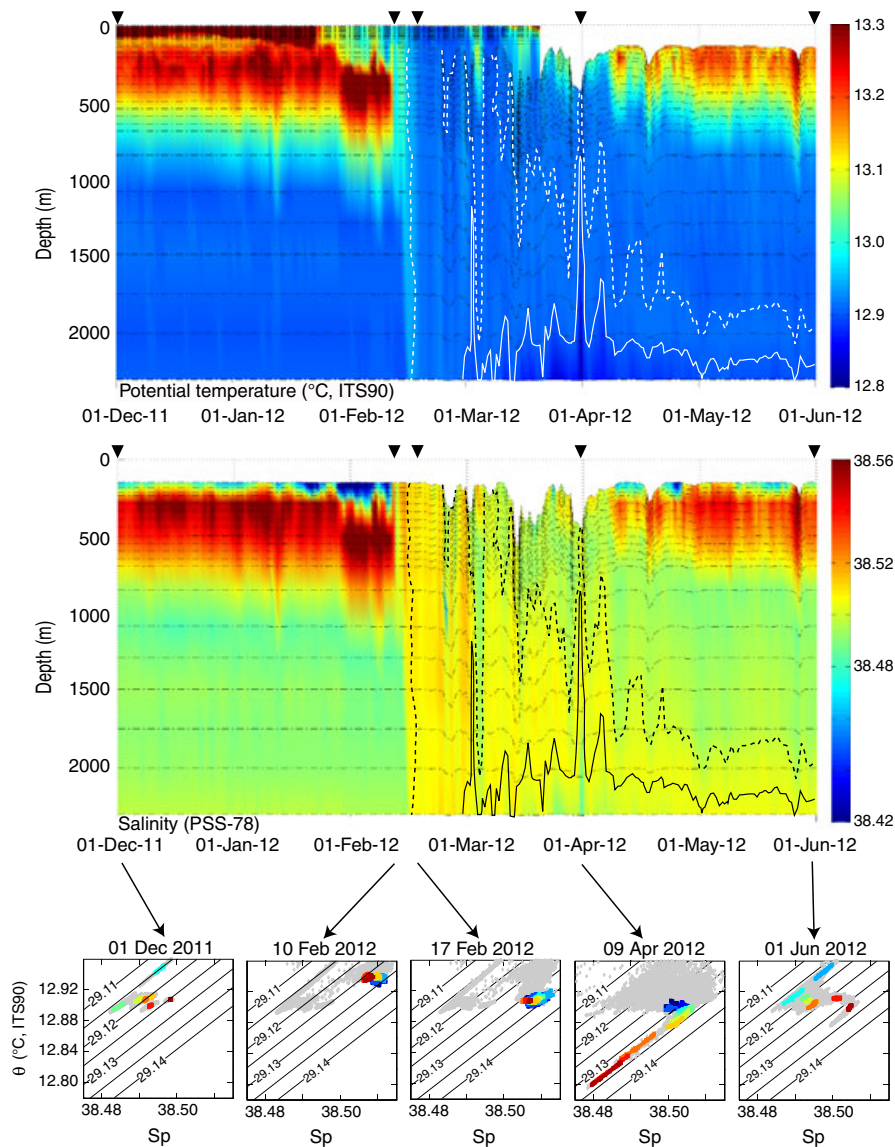


Figure 3. (a) Surface plot of temperature and salinity in the basin site (LION) between 1 December 2011 and 1 June 2012. The horizontal dashed-dotted lines indicated the depth of the sensors. The thick dashed line depicts the upper limit of water denser than 29.126 kg m^{-3} , and the thick solid the upper limit of bottom water denser than 29.13 kg m^{-3} and colder than 12.905°C . Theta-S plots (b) prior to the deep water formation, (c) at the time of arrival of the mixing layer at the bottom, (d) at the end of the strong mixing period, (e) during the apparition of colder and fresher bottom water, (f) during the spreading period. The colors correspond to the CTD measurements during a 12 h interval at the different levels (from the shallowest one in blue to the deepest one in dark red). The grey patterns represent the measurements during the month preceding the date of each diagram.

exported beyond 1000 m depth in the CCC amounted to $\sim 1,100 \text{ km}^3$, which was comparable to the volume estimated by *Ulses et al.* [2008] for the winter 2005. Assuming that the CCC exports half the total volume of dense shelf water, the mean flux to the basin corresponds to $0.07 \times 10^6 \text{ m}^3 \text{ s}^{-1}$, which is one order of magnitude less than the production of dense water by open-sea convection.

[22] The volumes of newly formed deep ($\sigma_\theta \geq 29.126 \text{ kg m}^{-3}$) and bottom ($\sigma_\theta \geq 29.13 \text{ kg m}^{-3}$ and $\theta \leq 12.905^\circ\text{C}$) waters that have not yet been advected or diffused out of the central part of the NW Mediterranean in summer 2012 (Figure 4a) were estimated at $14,000$ and $7,600 \text{ km}^3$, respectively. Albeit these values underestimated the actual volumes because the cruise did not cover the entire deep basin, the large increase of the volume of bottom water, with respect to that of

the dense water exported from the shelf, implied a large entrainment of ambient waters during its propagation down the slope and in the basin, including newly-formed deep water. Finally, these volumes were large enough to markedly alter the thermo-haline characteristics of the deep basin even more, hence contributing to amplify the Western Mediterranean Transition [CIESM, 2009].

4. Concluding Remarks

[23] Coastal and open-ocean deep convections are phenomena that ventilate the deep waters of the NW Mediterranean, and are potentially key processes for the climate variability. These observations allow to definitively conclude on the origin of the thermo-haline anomalies that

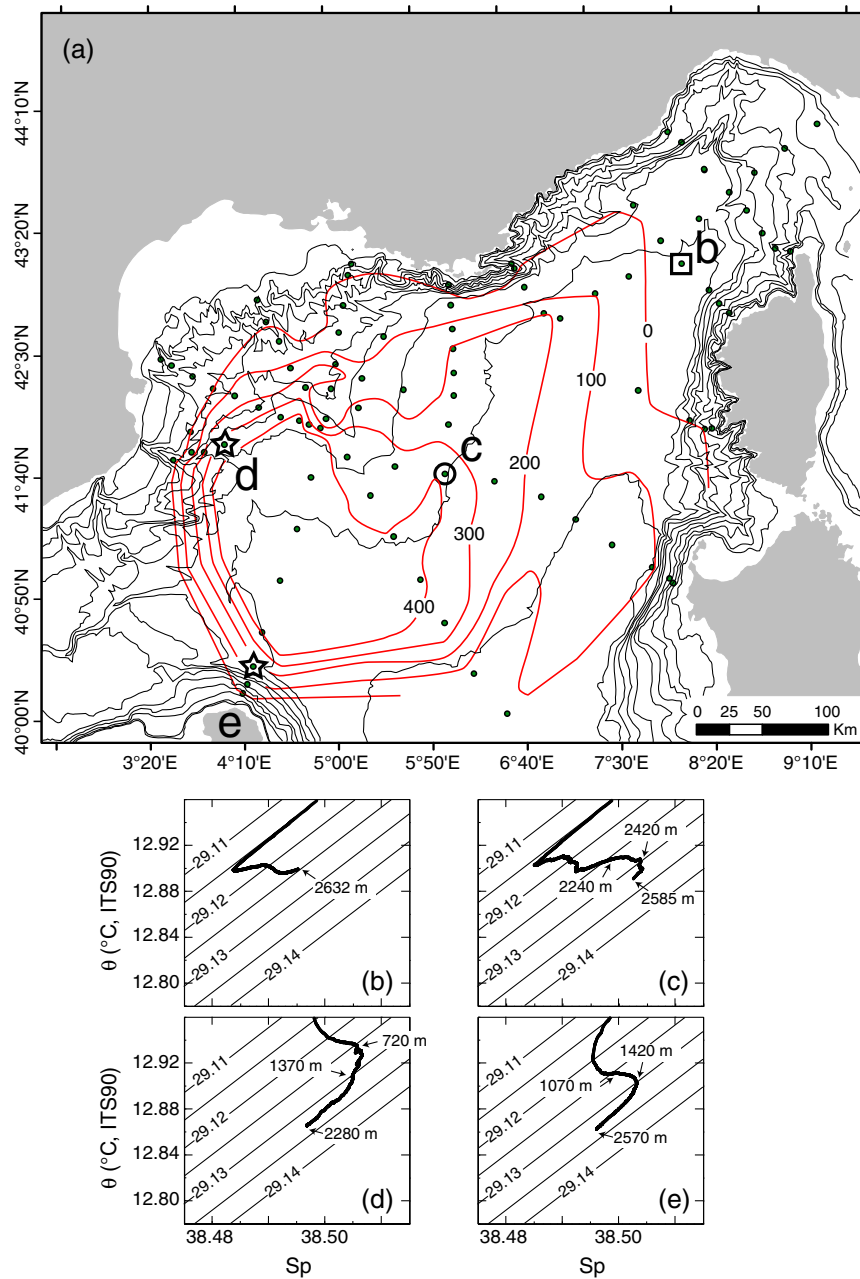


Figure 4. CTD stations performed during the summer cruise MOOSE (24 July to 8 August 2012), and cumulative thickness of the deep and bottom layers denser than 29.126 kg m^{-3} (a). Theta-S diagrams showing pre-2012 deep waters (square, b) and newly-formed ones (circle, c). Theta-S diagrams of the two peculiar stations (stars, d and e) showing a bottom anomaly extending about 1100 m above the seabed (not used in the mapping of thickness of the deep and bottom layers). The numbers indicate depths of the upper limit of the deep and bottom layers, and of the seabed.

were repeatedly observed over the last 40 years in the GoL. Although the preconditioning is certainly a key factor, we showed that the combined formation of deep water of coastal and open-sea origin is likely related to peculiar large-scale atmospheric circulation patterns. This study provides a first quantitative benchmark and, in particular, useful estimates of spatial and temporal scales associated with these ventilation mechanisms. This reference case can contribute to improve the capacity of the numerical ocean models that do not yet well reproduce deep convections for thorough analyses of their impact on the long-term variability of the WMDW.

[24] **Acknowledgments.** We acknowledge sponsorship from PERSEUS (FP7-OCEAN-2011-3-287600), SOERE-MOOSE, MISTRALS (MERMeX, HyMeX), CNRM/CMM (Météo France), HYDROCHANGE, ReDEco (CTM2008-04973-E), GRACCIE-CONSOLIDER (CSD2007-00067), and DOS MARES (CTM2010-21810-C03-01).

References

- Béthoux, J. P., X. Durrieu de Madron, F. Nyffeler, and D. Tailliez (2002), Deep water in the western Mediterranean: peculiar 1999 and 2000 characteristics, shelf formation hypothesis, variability since 1970 and geochemical inferences, *J. Mar. Syst.*, 33–34, 117–131.
- Canals, M., P. Puig, X. Durrieu de Madron, S. Heussner, A. Palanques, and J. Fabres (2006), Flushing submarine canyons, *Nature*, 444, 354–357.

- Cassou, C., M. Minvielle, L. Terray, and C. Périgaud (2010), A statistical-dynamical scheme for reconstructing ocean forcing in the Atlantic. Part I: weather regimes as predictors for ocean surface variable, *Clim. Dyn.*, 36(1–2), 19–39.
- CIESM (2009) Dynamics of Mediterranean deep waters. N°38 in CIESM Workshop monographs [F. Briand, Ed.], 132 pages, Monaco.
- Font, J., P. Puig, J. Salat, A. Palanques, and M. Emelianov (2007), Sequence of hydrographic changes in NW Mediterranean deep water due to the exceptional winter of 2005, *Sci. Mar.*, 71(2), 339–346. doi:10.3989/scimar.2007.71n2339.
- Josey, S.A., S. Somot, and M. Tsimplis (2011) Impacts of atmospheric modes of variability on Mediterranean Sea surface heat exchange. *J. Geophys. Res.*, doi:10.1029/2010JC006685.
- Kim, K., K. I. Chang, D. J. Kang, Y. H. Kim, and J. H. Lee (2008), Review of Recent Findings on the Water Masses and Circulation in the East Sea (Sea of Japan), *J. Oceanogr.*, 64, 721–735.
- L'Heveder, B., L. Li, F. Sevault, and S. Somot (2012), Interannual variability of deep convection in the Northwestern Mediterranean simulated with a coupled AORCM. *Climate Dynam.*, doi:10.1007/s00382-012-1527-5.
- Puig, P., et al. (2013), Thick bottom nepheloid layers in the western Mediterranean generated by deep dense shelf water cascading, *Prog. Oceanogr.*, doi: 10.1016/j.pocean.2012.10.003, in press.
- Quadfasel, D., B. Rudels, and K. Kurz (1988), Outflow of dense water from a Svalbard fjord into the Fram Strait, *Deep-Sea Res. I*, 35, 1143–1150.
- Schroeder, K., A. Ribotti, M. Borghini, R. Sorgente, A. Perilli, and G.P. Gasparini (2008), An extensive Western Mediterranean deep water renewal between 2004 and 2006. *Geophys. Res. Lett.*, 35, L18605, doi:10.1029/2008GL035146.
- Testor, P., and J. C. Gascard (2006), Post-convection spreading phase in the Northwestern Mediterranean Sea, *Deep-Sea Res. I*, 53, 869–893.
- Ulses, C., C. Estournel, P. Puig, X. Durrieu de Madron, and P. Marsaleix (2008), Dense water cascading in the northwestern Mediterranean during the cold winter 2005. Quantification of the export through the Gulf of Lion and the Catalan margin. *Geophys. Res. Lett.*, 35, L07610, doi:10.1029/2008GL033257.